J Bioenerg Biomembr (2012) 44:51–60
DOI 10.1007/s10863-012-9411-x

Bromopyruvate mediates autophagy and cardiolipin degradation to monolyso-cardiolipin in GL15 glioblastoma cells

Magdalena Davidescu · Miriam Sciaccaluga · Lara Macchioni · Roberto Angelini · Patrizia Lopalco · Maria Grazia Rambotti · Rita Roberti · Angela Corcelli · Emilia Castigli · Lanfranco Corazzi

Received: 28 December 2011 / Accepted: 18 January 2012 / Published online: 9 February 2012

Abstract The GL15 glioblastoma cell line undergoes viability loss upon treatment with bromopyruvate. The biochemical mechanisms triggered by the antiglycolytic agent indicate the activation of an autophagic pathway. Acridine orange stains acidic intracellular vesicles already 60 min after bromopyruvate treatment, whereas autophagosomes engulfing electron dense material are well evidenced 18 h later. The autophagic process is accompanied by the expression of the early autophagosomal marker Atg5 and by LC3-II formation, a late biochemical marker associated with autophagosomes. In agreement with the autophagic route activation, the inhibitory and the activator Akt and ERK signaling pathways are depressed and enhanced, respectively. In spite of the energetic collapse suffered by bromopyruvate-treated cells, MALDI-TOF mass spectrometry lipid analysis does not evidence a decrease of the major phospholipids, in accordance with the need of phospholipids for autophagosomal membranes biogenesis. Contrarily, mitochondrial cardiolipin decreases, accompanied by monolyso-cardiolipin formation and complete cytochrome c degradation, events that could target mitochondria to autophagy. However, in our experimental conditions cytochrome c degradation seems to be independent of the autophagic process.

Keywords Bromopyruvate · Glioblastoma cells · Autophagy · Cytochrome c · Cardiolipin · Lyso-cardiolipin

M. Davidescu · L. Macchioni · R. Roberti · L. Corazzi (✉)
Department of Internal Medicine, Laboratory of Biochemistry,
University of Perugia,
Via del Giochetto,
06122 Perugia, Italy
e-mail: corazzi@unipg.it

M. Sciaccaluga
Istituto Pasteur-Fondazione Cenci Bolognetti
and Department of Physiology and Pharmacology,
Sapienza University of Rome,
Rome, Italy

R. Angelini · A. Corcelli
Department of Basic Medical Sciences,
University of Bari "Aldo Moro",
Bari, Italy

P. Lopalco
IMM-CNR, Institute for Microelectronics and Microsystems,
National Research Council,
Lecce, Italy

M. G. Rambotti
Department of Experimental Medicine and Biochemical Sciences,
University of Perugia,
Perugia, Italy

A. Corcelli
IPCF-CNR, Institute for Chemical-Physical Processes,
National Research Council,
70124 Bari, Italy

E. Castigli
Department of Cellular and Environmental Biology,
University of Perugia,
Perugia, Italy

Abbreviations

CL	cardiolipin
Cyt c	cytochrome c
DMEM	Dulbecco's modified Eagle's medium
GSK-3β	glycogen synthase kinase-3 β
MLCL	monolyso-cardiolipin
PA	phosphatidic acid
PC	phosphatidylcholine
PE	phosphatidylethanolamine
PI	phosphatidylinositol
PS	phosphatidylserine
SM	sphingomyelin
TEM	transmission electron microscopy

Introduction

In the sixties, bromopyruvate was used as a site-specific alkylating agent for 2-keto-3-deoxy-6-phosphogluconic aldolase, an enzyme catalyzing the reversible condensation of pyruvate and D-glyceraldeheyde-3-phosphate, and as a reactive probe in kinetic and stereochemical studies (Meloche 1967; Meloche et al. 1972). More recently, it has been discovered that bromopyruvate inhibits the hexokinase of the VX2 tumor implanted in the liver for studying hepatocellular carcinomas (Ko et al. 2004). This tumor exhibits a high glycolytic glucose catabolic rate and contains elevated levels of hexokinase bound to mitochondria (Pedersen 1978; Bustamante et al. 1981). These findings have been related to the common feature of many advanced cancers to possess an enhanced capacity to metabolize glucose to lactic acid. Treatment with the alkylating agent bromopyruvate, that acts as an apparently nontoxic cellular energy blocker, eradicated a large liver tumor grown in rats (Ko et al. 2001, 2004). In several tumor cell lines, bromopyruvate induced cell death, although with a variety of biochemical mechanisms (Xu et al. 2005; Kim et al. 2008; Yun et al. 2009; Pereira da Silva et al. 2009; Qin et al. 2010). The efficacy of bromopyruvate therapy in depleting ATP in cancer cells may be due to the fact that tumor cells rely preferentially on anaerobic glycolysis for the synthesis of ATP rather than on oxidative phosphorylation, even when oxygen is available (Cairns et al. 2011; Levine and Puzio-Kuter 2010).

Glucose metabolism has been investigated in the search of treatments of glioblastoma cells, the most common and malignant central nervous system tumor. Impairment of mitochondrial respiration and enhanced resistance to mitochondrial apoptosis are main features of these cells (Joy et al. 2003). However, glucose withdrawal was found to induce oxidative stress followed by apoptosis in glioblastoma, but not in normal human astrocytes (Jelluma et al. 2006). Glioblastoma cells, although very resistant to apoptosis, undergo autophagy in response to various anticancer therapies (Krakstad and Chekenya 2010; Lefranc and Kiss 2006; Lefranc et al. 2007). Two main pathways abnormally activated in glioblastoma cells are deeply involved in the control of autophagy: the Akt/mTOR and the ERK1/2 signalling pathways regulate the progress of autophagy negatively and positively, respectively (Kondo et al. 2005; Aoki et al. 2007; Eom et al. 2010; Wang et al. 2009).

In GL15 glioblastoma cells, apoptosis was induced following an imbalanced control of cell cycle progression (Castigli et al. 2000, 2006). Moreover, alteration of cardiolipin (CL) synthesis in palmitate-treated cells resulted in weakening of cytochrome c (cyt c) binding to the inner mitochondrial membrane, cyt c release outside mitochondria, and triggering of the subsequent apoptotic cascade (Buratta et al. 2008). A peculiar feature of GL15 cells is the tight binding of cyt c to the inner mitochondrial membrane that enables cells to escape the cyt c-triggered apoptotic pathway. In a recent paper we have shown that GL15 cell starvation produced by bromopyruvate forces these cells to switch to respiration for their energy supply (Macchioni et al. 2011a). Thus, cyt c is targeted for degradation, possibly due to acquired peroxidase activity (Macchioni et al. 2011b). This process is specific and impairs the apoptotic cyt c cascade, although cells are committed to die. Bromopyruvate caused $\Delta\psi_m$ and MTT collapse, ATP decrease, and cell viability loss, without involving apoptotic or necrotic pathways, but suggesting an autophagic pathway.

In this work we have investigated this matter carefully and discovered that bromopyruvate triggers an autophagic process. The Endoplasmic reticulum plays an active role during autophagosome bilayer formation. Therefore, phospholipid analysis of GL15 cells following bromopyruvate treatment was performed. Despite cellular energy collapse and an activated degradation processes, the pattern of the major phospholipid classes was not significantly affected. Contrarily, the mitochondrial phospholipid CL underwent degradation to monolyso-cardiolipin (MLCL).

Materials and methods

Chemicals Bromopyruvic acid, acridine orange, menadione, N-acetyl-cysteine, phosphatase inhibitor cocktail II, protease inhibitor cocktail, LC3 rabbit polyclonal antibody, and β-tubulin mouse monoclonal antibody were obtained from Sigma (Italy). Cyt c mouse monoclonal antibody, APG-5(C-1) (Atg5) mouse monoclonal antibody, goat anti-mouse HRP-conjugated IgG, and rabbit anti-goat HRP-conjugated IgG were from Santa Cruz Biotechnology; glycogen synthase kinase-3 β (GSK-3β) (27C10) rabbit monoclonal antibody, which detects endogenous levels of

total GSK-3β protein, phospho-GSK-3β (Ser9) rabbit antibody, which detects endogenous levels of GSK-3β only when phosphorylated at serine 9, phospho-Akt (Ser473) rabbit monoclonal antibody, which detects endogenous levels of Akt only when phosphorylated at Ser473, p44/42 MAPK rabbit monoclonal antibody, and anti-phospho-p44/42 MAPK (ERK1/2) (Thr202/Tyr204) mouse monoclonal antibody were from Cell Signaling Technology; goat anti-rabbit and goat anti-mouse HRP-conjugated IgG were from Pierce. 9-Aminoacridine hemihydrate was purchased from Acros Organics (Morris Plains, NJ). The following commercial glycerophospholipids (used as standards): 1,1′,2,2′-tetratetradecanoyl cardiolipin, 1,1′2,2′-tetra-(9Z-octadecenoyl) cardiolipin, 1,2-ditetradecanoyl-*sn*-glycero-3-phosphate, 1,2-ditetradecanoyl-*sn*-glycero-3-phospho-(1′-rac-glycerol), 1,2-ditetradecanoyl-*sn*-glycero-3-phospho-L-serine, 1,2-di-(9Z-hexadecenoyl)-*sn*-glycero-3-phosphoethanolamine, were purchased from Avanti Polar Lipids, Inc. (Alabaster, AL). All organic solvents used in extraction and mass spectrometry analysis were commercially distilled and of the highest available purity and were purchased from Sigma Aldrich, J.T. Baker or Carlo Erba.

Cell culture and treatments GL15 glioblastoma cells were grown as previously described (Buratta et al. 2008). The cells were trypsinized, plated in 6-well plates (2×10^5 cell per well), and incubated for 3 days at 37 °C in a 5% CO_2 humidified atmosphere to obtain semi-confluent cells. Medium was removed and cells were incubated for 18 h in serum-free DMEM in the presence of a buffered solution of bromopyruvate (0–100 μM, pH 7.4). Where indicated, menadione (10 μM) or N-acetyl-cysteine (4 mM) were added. After the treatments, detached and trypsinized adherent cells were combined for subsequent analysis.

Western blot analysis Whole-cell lysates (50 μg protein) of control and treated GL15 cells were analyzed by Western blot for cyt c and Atg5, using nitrocellulose membranes, and for LC3, using PVDF membranes. To investigate the effect of bromopyruvate treatment in the Akt and ERK1/2 pathways, GL15 cells were serum starved for 30 min in the presence or absence of 80 μM bromopyruvate. Cell cultures were washed with PBS and scraped with 62.5 mM Tris–HCl (pH 6.8), 2 mM EDTA, 0.5% Triton X-100, phosphatase inhibitor cocktail II, protease inhibitor cocktail, and 2% SDS. Western blot analysis of phosphorylated Akt, GSK3β, and ERK1/2, and of total GSK3β and ERK1/2 was performed by using nitrocellulose membranes and the specific antibodies, following the instructions of the manufacturer. Images of immunoblots were acquired using the VersaDoc 1000 imaging system and quantified using Quantity One software (BioRad).

Acridine orange staining of GL15 cells GL15 cells were grown in glass coverslips for 3 days, and serum starved for 60 min in the presence or absence of bromopyruvate. The cells were stained with 2 μg/ml acridine orange in phosphate buffered saline for 15 min at 37 °C and immediately analyzed with a fluorescence microscope (DMRB Leika).

Transmission electron microscopy Cells were examined by transmission electron microscopy (TEM) following standard procedures, with a Philips TEM 400 electron microscope.

Lipid extraction and analysis by TLC Lipids were extracted as described (Bligh and Dyer 1959). For the efficient recovery of CL, solvent mixtures were added with HCl (0.5 mM). Total lipids were quantified by phosphorus assay (Bartlett 1959). Phospholipid classes were separated by two-dimensional TLC. Lipids were visualized with Cu-acetate reagent, and individual band densities were integrated using Quantity One software (BioRad) (Macchioni et al. 2010).

Preparation of lipid samples in solution for MALDI-TOF mass spectrometry Total lipids of glioblastoma cells were extracted as described above with minor modifications (Lobasso et al. 2010); the extracts were carefully dried under N_2 before weighing and then dissolved in chloroform (10 mg/ml). Samples were prepared as previously described (Sun et al. 2008). Briefly, the total lipid extract was diluted from 20 to 200 μl with isopropanol/acetonitrile (60/40, by volume). Next, 10 μl of a diluted sample was mixed with 10 μl of 9-aminoacridine (10 mg/ml in isopropanol/acetonitrile, 60/40, by volume). An aliquot of the mixture (0.3 μl) was spotted on the MALDI target (Micro Scout Plate, MSP 96 ground steel target).

MALDI-TOF mass spectrometry MALDI-TOF mass spectra were acquired on a Bruker Microflex RLF mass spectrometer (Bruker Daltonics, Bremen, Germany). The system utilizes a pulsed nitrogen laser, emitting at 337 nm; the extraction voltage was 20 kV and gated matrix suppression was applied to prevent detector saturation. Ten thousand single laser shots (sum of 40×250) were averaged for each mass spectrum. The laser fluence was kept about 10% above threshold to have a good signal-to-noise ratio. All spectra were acquired in the reflector mode using the delayed pulsed extraction, both in the negative and positive ion mode. Spectral mass resolutions, signal-to-noise ratios, and peak areas were determined by the software for the instrument, "Flex Analysis 3.3.65" (Bruker Daltonics). A mix containing 1,1′,2,2′-tetratetradecanoyl cardiolipin, 1,1′2,2′-tetra-(9Z-octadecenoyl) cardiolipin, 1,2-ditetradecanoyl-*sn*-glycero-3-phosphate, 1,2-ditetradecanoyl-*sn*-glycero-3-phospho-(1′-rac-glycerol), 1,2-ditetradecanoyl-*sn*-glycero-3-phospho-L-serine, 1,2-di-(9Z-hexadecenoyl)-*sn*-glycero-3-

phosphoethanolamine was always spotted next to the sample as external standard and an external calibration was performed before each measurement; the mass range of the authentic standards is 590–1450 a.m.u.

Results

Autophagic response of GL15 cells to bromopyruvate treatment GL15 glioblastoma cells were treated with bromopyruvate for 18 h in the 0–100 μM concentration range. Previously, we observed a collapse of both MTT and mitochondrial membrane potential in the 70–80 μM range, accompanied by massive degradation of cyt c and Bax within mitochondria. ATP levels did not change up to 60 μM bromopyruvate and reached about 7% of the control in 80 μM bromopyruvate-treated cells (Macchioni et al. 2011a). Cyt c degradation following the treatment of GL15 cells with 80–100 μM bromopyruvate was confirmed in the experiments reported in Fig. 1.

Atg5 has been previously characterized as a protein specifically required for autophagy, representing an early autophagosomal marker. Atg5 was over expressed in the 50–60 μM bromopyruvate range and started to decline at 70 μM bromopyruvate. Autophagy was confirmed by the appearance of the truncated, PE-conjugated LC3 protein (LC3-II), a late autophagosomal marker, which was the only form present at 80 μM bromopyruvate (Fig. 1). The treatment of cells with the free radical inducer menadione caused disappearance of cyt c. However, no LC3-II protein was detected, suggesting the absence of an autophagic process. N-acetyl-cysteine counteracted cyt c degradation in bromopyruvate-treated cells and attenuated the formation of the LC3-II protein (Fig. 1). However, it is noteworthy that bromopyruvate acts as an alkylating agent towards the -SH groups of N-acetyl-cysteine, thus resulting less effective.

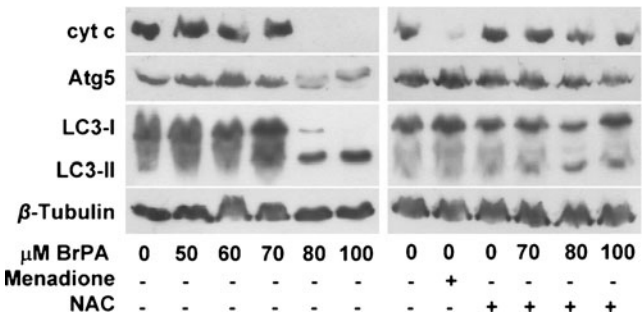

Fig. 1 Bromopyruvate-treated GL15 cells express autophagy markers. Cells were treated for 18 h with increasing concentrations of bromopyruvate (BrPA) in the absence or in the presence of N-acetyl-cysteine (NAC), or with 10 μM menadione. Western blot analysis of the autophagy markers Atg5 and LC3 proteins was performed. The truncated, autophagosome associated LC3-II form is present only at 80 and 100 μM bromopyruvate. The extent of cyt c degradation was evaluated to verify the effectiveness of bromopyruvate treatment (see ref. Macchioni et al. 2011a). Representative blots are shown

We have previously demonstrated the abnormal activation of Akt and ERKs in GL15 cells (Castigli et al. 2000, 2006; Sciaccaluga et al. 2010) and therefore we investigated the effect of bromopyruvate on Akt and ERK activity by evaluating the expression of their phosphorylated forms. Moreover, since the inhibition of glycogen synthase kinase-3β (GSK3β) by Akt is involved in the association of hexokinase II to VDAC in the mitochondria (Pastorino et al. 2005; Pastorino and Hoek 2008; Pedersen 2007, 2008; Mathupala et al. 2006), we also evaluated the possibility that bromopyruvate activates GSK3β, constitutively inhibited in GL15 cells (Macchioni et al. 2011a). After 30 min of treatment with 80 μM bromopyruvate, the activity of Akt was significantly inhibited, as demonstrated by the decrease of pAkt. Accordingly, pGSK3β was also reduced, resulting in its activation. At the same time an increase of the active pERKs was observed (Fig. 2). This result is in agreement with the induction of an autophagic pathway in bromopyruvate-treated cells.

Bromopyruvate-treated GL15 cells were stained with acridine orange to detect acidic vesicular organelles. As early as 60 min after 60 μM bromopyruvate treatment, cells with acidic vesicular organelles were observed (Fig. 3b), while control cells showed the classical punctuate orange staining of acidic compartments (Fig. 3a).

GL15 cells were analysed by TEM after treatment with 80 μM bromopyruvate. In Fig. 3, representative electron micrographs show the presence of autophagic bodies engulfing electron dense material in the cytoplasm of treated (Fig. 3c), but not of untreated cells (Fig. 3d). These data confirm that starvation produced by bromopyruvate treatment of GL15 cells evolves towards autophagy. Interestingly, intact mitochondria were detectable in treated cells (Fig. 3e), suggesting that this organelle is not massively engulfed in autophagosomes.

Analysis of phospholipids of GL15 cells after bromopyruvate treatment Phospholipids assume a very important role in membrane biogenesis during autophagic processes; therefore, lipidomics of GL15 cells was studied after bromopyruvate treatment. First, phospholipids were separated by two-dimensional TLC (Fig. 4). The percent of individual phospholipid classes is reported in Table 1. In spite of the dramatic metabolic changes suffered by cells treated with 80 μM bromopyruvate, no changes were detected for the major phospholipids. Contrarily, CL content decreased significantly.

Second, MALDI-TOF mass spectrometry lipid profile of GL-15 cells was analyzed. Mass spectra of the total lipid

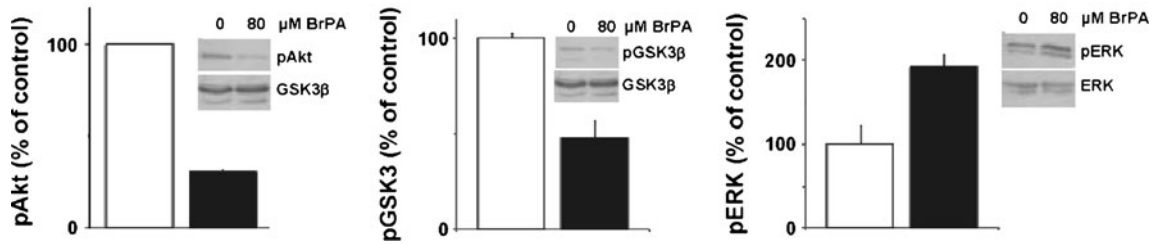

Fig. 2 Effect of bromopyruvate on Akt and ERKs pathways. GL15 cells were serum starved for 30 min in the presence or absence of 80 μM bromopyruvate (BrPA). Immunolabeling of phosphorylated Akt, GSK3β, and ERK1/2 was performed. For loading normalization total GSK3β and ERK were used. Histograms report density ratios between phosphorylated and total forms as percent of the treated (*black columns*), compared to control (*open columns*). Data are the mean ± SD from three experiments. Representative blots are shown

extracts of control and 80 μM bromopyruvate-treated cells, acquired in the negative ion mode using 9-aminoacridine as matrix are shown in Fig. 5 (*m/z* range, 600–1000) and Fig. 6 (*m/z* range, 1000–1500). The signals in the spectra attributable to the negative $[M-H]^-$ molecular ions of phospholipids and sphingolipids are collected in Table 2. The peaks can be grouped in 3 main *m/z* ranges: a) *m/z* 650–1000, major phospholipids; b) *m/z* 800–1400, attributable to glycosphingolipids; c) *m/z* 1350–1500, CLs. In the range of major phospholipids (Fig. 5), the peaks at *m/z* 673.6 and 701.6

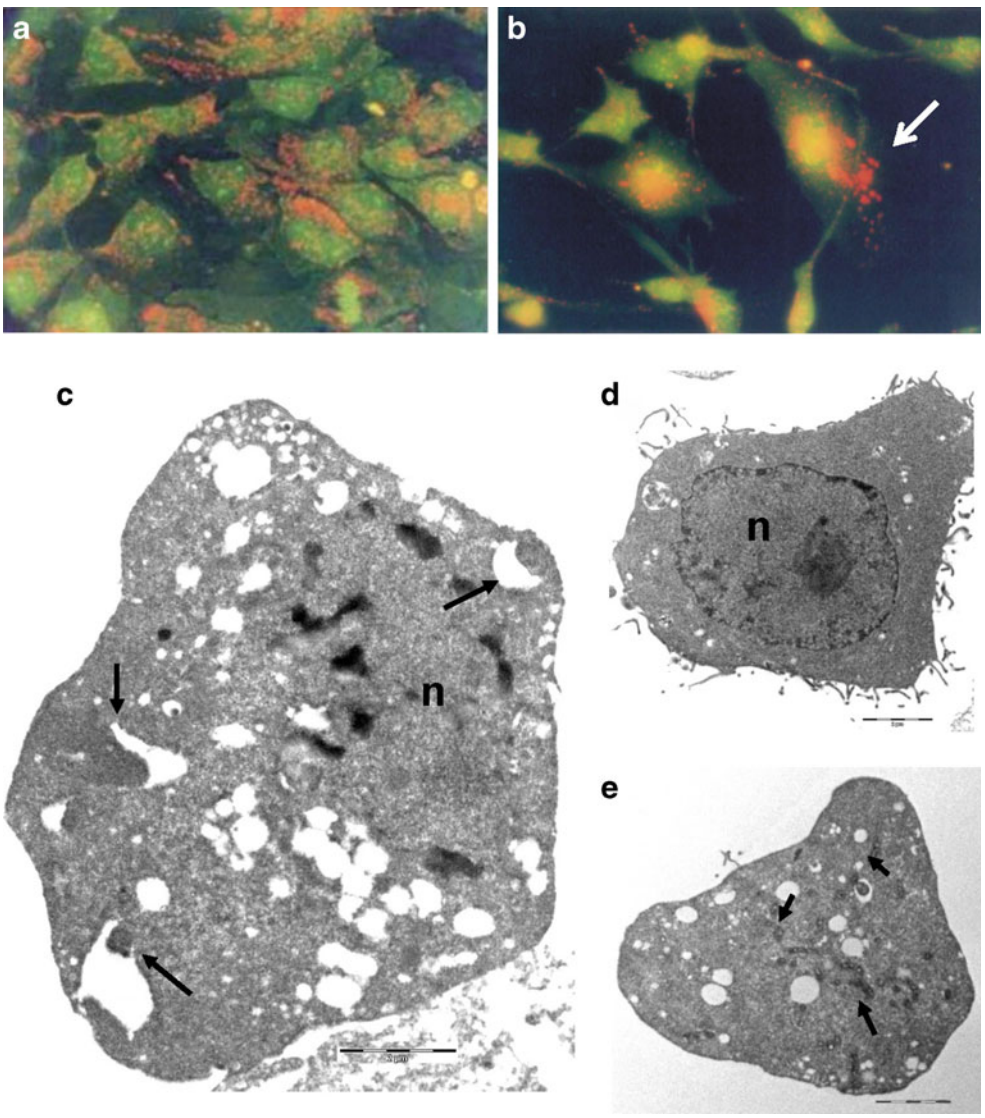

Fig. 3 Detection of autophagosomes in bromopyruvate-treated GL15 cells. **a** and **b** Acridine orange staining after 60 min treatment with 60 μM bromopyruvate. Control cells (**a**) show the classical punctuate orange staining of acidic compartments, while vesicular acidic organelles are evident in treated cells (**b**, *white arrow*). Original magnification, 400x. **c-e** Ultrastructural analysis of cells by TEM. Electron micrographs show the presence of autophagic vesicles engulfing electron dense material in 80 μM bromopyruvate-treated cells (**c**, *black arrows*) but not in the untreated cells (**d**). Intact mitochondria are evident in treated cells (**e**, *black arrows*). n: nucleus. Bars: 2 μm

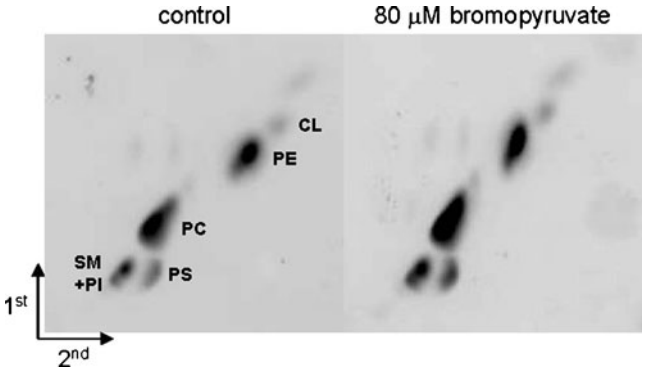

Fig. 4 Representative 2D-TLC phospholipid profile of control and bromopyruvate-treated GL15 cells. Lipid extracts were separated by two-dimensional TLC with (1st) chloroform/methanol/1.6 M ammonia (70:30:5, by volume) and (2nd) chloroform/methanol/acetone/acetic acid/water (75:15:30:15:7.5, by volume). Lipids were visualized with Cu-acetate reagent and individual band densities were integrated for quantification (see Table 1). *PE* phosphatidylethanolamine; *PC* phosphatidylcholine; *PS* phosphatidylserine; *CL* cardiolipin; *PI* phosphatidylinositol; *SM* sphingomyelin

can be attributed to phosphatidic acid (PA) 34:1 and 36:1, respectively; the peaks at *m/z* 742.6 and 774.6 are attributable to phosphatidylethanolamine (PE) 36:2 and 38:0, respectively; the peak at *m/z* 788.6 is assigned to phosphatidylserine (PS) 36:1; various species of phosphatidylinositol (PI) are present at *m/z* 835.6 (34:1), 861.7 (36:2), 885.7 (38:4), and 887.7 (38:3). In the range of glycosphingolipids a number of peaks is present; the major peak is at *m/z* 1261.9 (Fig. 6) and is attributed to a ganglioside (LM_ID: LMSP0601AJ07, systematic name: NeuAcα2-3Galβ1-4Glcβ-Cer(d18:1/24:1(15Z)). In the CLs range (Fig. 6) a large number of peaks is present, attributable to CLs of different chain length; major peaks at *m/z* 1400.1, 1428.2, and 1454.2 are attributed to CL 68:4, 70:4, and 72:5, respectively. In the MLCL range, peaks are present only in the treated cells (Fig. 6). Peaks at *m/z* 1163.9 and 1191.9 can be attributed to MLCL 52:3 and 54:3, respectively. Figure 7 shows the MALDI-TOF mass spectra of the total lipid extracts of GL-15 cells acquired in the positive ion mode, using 9-aminoacridine as matrix. The major peaks have been attributed to phosphatidylcholine (PC) species of different acyl chain length as follows: *m/z* 760.6, PC 34:0 and *m/z* 786.6, PC 36:1. Control and bromopyruvate-treated cells showed the same peak profile.

The only relevant differences between control and bromopyruvate-treated cells are in the negative ion mode lipid profile, *m/z* range 1000–1500, showing a reduction in the CLs content and a concomitant production of their degradation products MLCLs in treated cells (Fig. 6). This result confirms the data obtained by TLC analysis reported in Table 1.

Table 1 Glycerophospholipid pattern in bromopyruvate-treated GL15 cells

	Control	Treated
Total lipid P (nmol/mg protein)	562.2±22.7	575.0±32.1
%		
PE	24.6±4.4	24.6±5.2
PC	44.4±4.1	42.8±5.3
PS	8.6±3.3	10.8±0.6
CL	5.6±0.6	3.8±0.4*
PI+SM	16.3±2.2	17.3±1.1

Lipids from cells incubated 18 h with 80 μM bromopyruvate were extracted, purified, and quantified as described in Materials and methods. Phospholipid composition is expressed as mol percent. Abbreviations are as in legend to Fig. 4. Data are the means ± SD (5 determinations). * Significance reached, $p<0.05$ (Student's *t*-test)

Discussion

Bromopyruvate is a potent antiglycolytic, able to induce severe ATP reduction and viability loss in many cancer cell lines, including GL15 glioblastoma cells (Macchioni et al. 2011a). A variety of biochemical mechanisms by which this antiglycolytic agent leads cells to die have been described in different cell types (Xu et al. 2005; Kim et al. 2008; Yun et al. 2009; Pereira da Silva et al. 2009; Qin et al. 2010). In this paper, we demonstrate that bromopyruvate triggers an autophagic process in GL15 glioblastoma cells. Since the endoplasmic reticulum may play a significant function in autophagosome formation, by providing phospholipids for autophagosomal membranes, lipidome of GL15 cells has been analyzed.

The process of autophagy is characterized as a degradation of proteins and organelles into membrane vesicles, termed autophagosomes, and it is dependent on several proteins for its progression (Jiang et al. 2009). Atg5 functions as substrate for the autophagy protein Atg12. These proteins bind together to form Atg12/Atg5 conjugates, which are required for the progression of autophagy in its early steps (Hailey et al. 2010). LC3 is the most used biochemical marker to monitor autophagic flux. LC3-II, the PE conjugated form of LC3-I, is the only protein marker that is reliably associated with a complete autophagosome (Klionsky et al. 2008). We found that at 60 μM bromopyruvate Atg5 was increased, compared to control (Fig. 1), whereas no LC3-II formation was observed, indicating that the autophagic pathway was in its early steps. By increasing bromopyruvate, the decline of Atg5 was accompanied by LC3-II formation, demonstrating the evolution of the autophagic process (Fig. 1). Indeed, acidic vesicle compartments were well evident in some cells already after 60 min treatment with 60 μM bromopyruvate (Fig. 3b), whereas mature, active

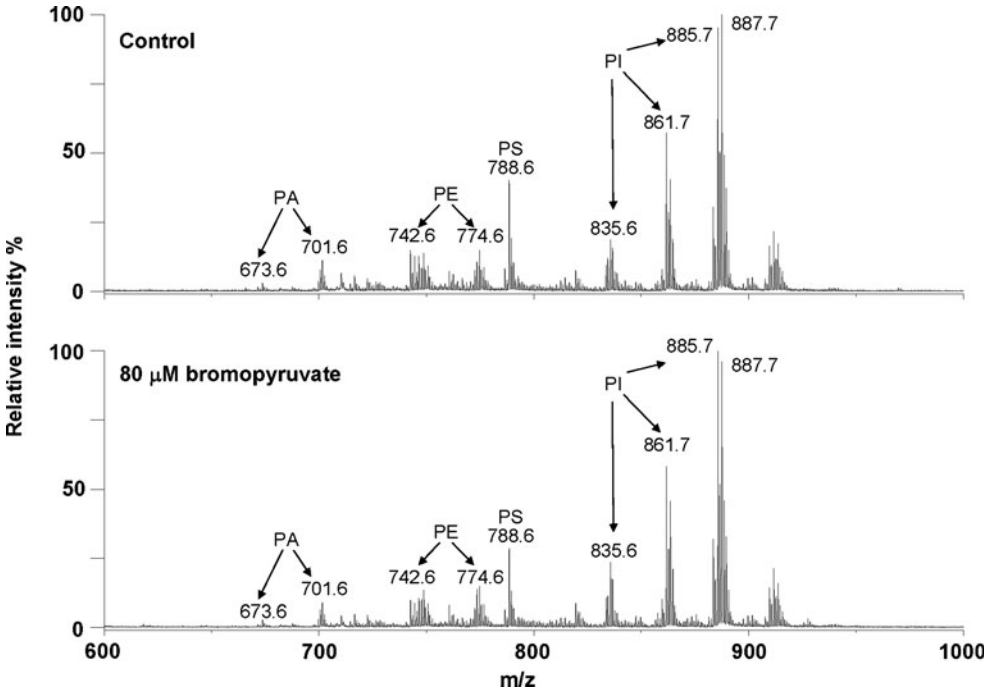

Fig. 5 MALDI-TOF mass spectrometry lipid profiles of control and bromopyruvate-treated GL-15 cells in the *m/z* range 600–1000. Peaks, acquired in the negative ion mode using 9-aminoacridine as the matrix, are attributable to PA, PE, PS, and PI. Phospholipid abbreviations are as in legend to Fig. 4. A detailed identification of peaks is reported in Table 2

autophagosomes appeared after 18 h treatment with 80 μM bromopyruvate (Fig. 3c).

The abnormal activation of Akt and ERKs is a feature of GL15 cells (Castigli et al. 2000, 2006; Sciaccaluga et al. 2010). Moreover, Akt/mTOR and ERK1/2 pathways are involved in the regulation of autophagy progression in glioblastoma cells (Kondo et al. 2005; Aoki et al. 2007; Eom et al. 2010; Wang et al. 2009). Our results demonstrate that bromopyruvate treatment favors the autophagic route since it depresses the inhibitory Akt while enhancing the activator ERKs (Fig. 2). As expected, Akt inhibition resulted in the activation of GSK3β. It has been demonstrated that the activation of GSK3β disrupts the binding of hexokinase II to mitochondria by phosphorylating VDAC (Pastorino et al.

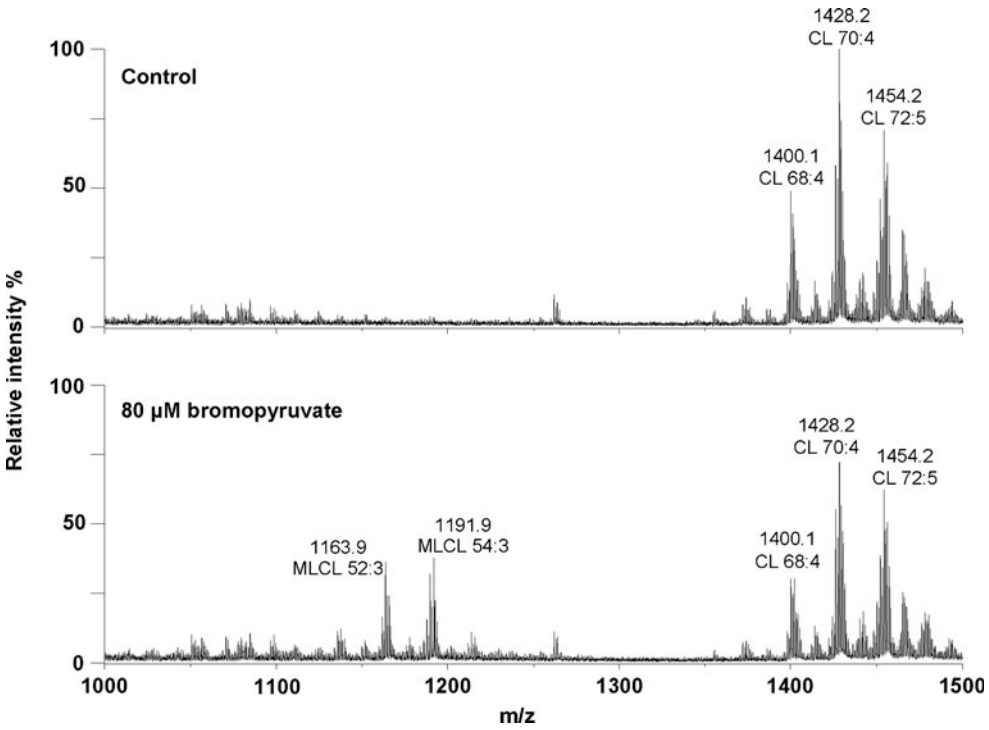

Fig. 6 MALDI-TOF mass spectrometry lipid profiles of control and bromopyruvate-treated GL-15 cells in the *m/z* range 1000–1500. Peaks were acquired in the negative ion mode using 9-aminoacridine as the matrix. CL peaks are in the *m/z* range 1300–1500. MLCL peaks are in the *m/z* range 1100–1250 (see also Table 2). 100% of relative intensity is assigned to the peak at 1428.2 in the lipid profile of control cells. The spectra show the presence of MLCLs and the concomitant reduction of CL content in GL-15 cells treated with bromopyruvate. The peak at 1262.0 could be attributed to a ganglioside, basing on lipid maps database: LM_ID: LMSP0601AJ07

Table 2 Signals in the spectra attributable to the negative $[M-H]^-$ molecular ions of phospholipids and sphingolipids

m/z value	Assignment $[M-H]^-$
673.6	PA 34:1
701.6	PA 36:1
742.6	PE 36:2
774.6	PE 38:0
788.6	PS 36:1
835.6	PI 34:1
861.7	PI 36:2
885.7	PI 38:4
887.7	PI 38:3
1262.0	ganglioside
1163.9	MLCL 52:3
1191.9	MLCL 54:3
1400.1	CL 68:4
1428.2	CL 70:4
1454.2	CL 72:5

PA phosphatidic acid; *MLCL* monolyso-cardiolipin; other abbreviations as in legend to Fig. 4

2005; Pastorino and Hoek 2008; Pedersen 2007, 2008; Mathupala et al. 2006). Thus, bromopyruvate should weaken the tight binding of HKII and VDAC in GL15 cells.

In this cell line, characterized by a scarce propensity to use the respiratory chain substrates of Complex I, a dramatic energy collapse was produced by bromopyruvate above a well defined concentration threshold (Macchioni et al. 2011a). A peculiar event that accompanies the energy collapse is the intra-mitochondrial degradation of cyt c, a protein not only involved in respiration (Vladimirov et al. 2006). We reported that ROS produced in GL15 cells after bromopyruvate or menadione treatment could be responsible for the intra-mitochondrial cyt c degradation (Macchioni et al. 2011a). However, autophagy was detected in bromopyruvate-, but not in menadione-treated cells (Fig. 1). Therefore, cyt c disappearance should not be directly related to the autophagic process. Moreover, mitochondrial ROS should not be obligatory for the induction of autophagy in GL15 glioblastoma cells. Our findings are in agreement with a recent study in cyt c deficient HeLa cells, where autophagy was induced by staurosporine, even though ROS were not detected (Jiang et al. 2011). However, this is a controversial point, since other authors claim that ROS are involved in the regulation of autophagy (Kirkland et al. 2002; Botti et al. 2006; Chen et al. 2008).

Until very recently, autophagic activity was studied in terms of protein and organelle recycling, neglecting connections with phospholipids metabolism. A recent report demonstrated that an increased de novo phospholipid synthesis is coupled with autophagosome formation (Girardi et al. 2011). Phospholipids newly formed in the endoplasmic reticulum are the main source of membrane components for autophagosome. Particularly, the enhanced synthesis of PE by the CDP-ethanolamine pathway is required for PE lipidation of LC3-I to form LC3-II (Girardi et al. 2011). Alternatively, under starvation conditions, the PE necessary for autophagosome biogenesis is supplied by mitochondria through PS decarboxylase (Hailey et al. 2010). In this context, energy supply is required for lipid biosynthesis. We observed that, in spite of the energetic collapse suffered by GL15 cells following 80 μM bromopyruvate treatment, total phospholipid content did not change in treated, compared to

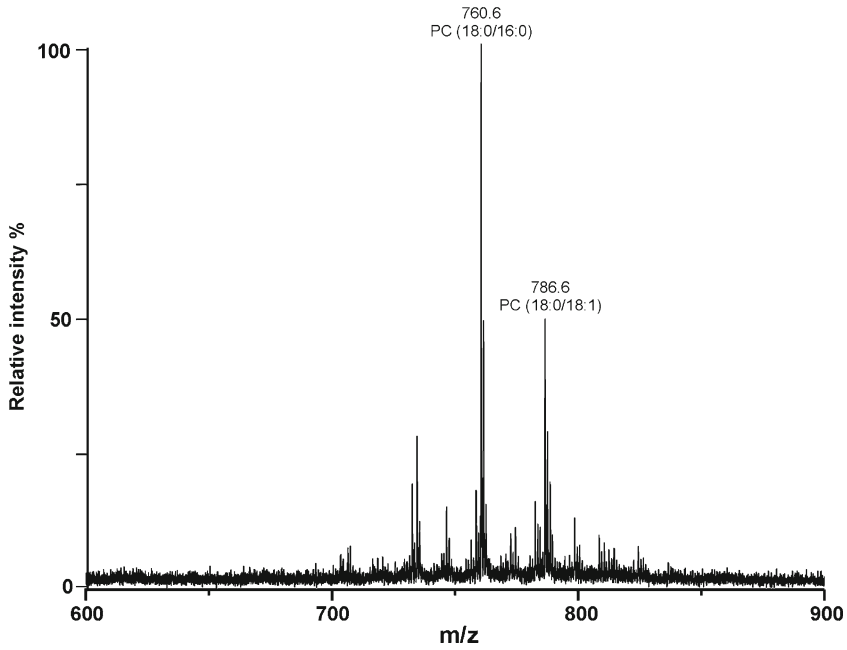

Fig. 7 MALDI-TOF mass spectrometry lipid profile of control GL-15 cells, acquired in positive ion mode. Phosphatidylcholines (PC) have been detected in the positive mode using 9-aminoacridine as the matrix. Major peaks at *m/z* 760.6 and 786.6 are assigned to PC (18:0/16:0) and PC (18:0/18:1), respectively

control cells, even though a significant CL decrease was measured (Table 1 and Fig. 6). Therefore, the maintenance of the phospholipid set should be sustained by the residual ATP level (Macchioni et al. 2011a). MALDI-TOF mass spectrometry analysis of treated, compared to control cells, confirmed that no significant modifications affected the major glycerophospholipids. Contrarily, the decrease of CL content was balanced by MLCL formation (Fig. 6). The presence of MLCL in treated, but not in control cells, may be considered a specific feature of phospholipid pattern modification in bromopyruvate-treated GL15 cells. CL localizes in the inner mitochondrial membrane, supports the anchorage of cyt c, and regulates mitochondrial functions (Zhang et al. 2002). Therefore, the contemporarily MLCL formation (Fig. 6) and cyt c degradation (Fig. 1) may be considered a signal of deep alteration and mitochondrial impairment in bromopyruvate-treated cells. MLCL formed in treated cells may be the result of an enhanced activity of mitochondrial phospholipase A_2 or an increased CL hydroperoxidation (Sorice et al. 2004). This second possibility is consistent with ROS production detected in bromopyruvate-treated GL15 cells due to cyt c peroxidase activity (Macchioni et al. 2011a). A direct correlation between cyt c degradation, MLCL formation, and triggering of the autophagic process could be hypothesized, although intact, not engulfed, mitochondria are present in treated cells (Fig. 3e).

Our previous studies reported the high potentiality of bromopyruvate to mediate GL15 glioblastoma cell death. Here, by means of biochemical markers and morphological studies, we demonstrate that cell death occurs through an autophagic pathway. The maintenance of the cell phospholipid panel contributes to sustain autophagosome formation. Bromopyruvate deeply affects the mitochondrial compartment by causing complete degradation of cyt c and breakdown of CL to MLCL, events that could address mitochondria to the autophagic process, although in our experimental conditions autophagy and cyt c degradation seem to be independent events.

Acknowledgements The authors gratefully acknowledge funds of Fondazione Cassa di Risparmio di Perugia (Project 2011.0184.021) and of the Laboratory Sens&Micro LAB Project (POFESR 2007–2013, code number 15) of Apulia Region. We thank Carlo Ricci for skillful technical assistance.

References

Aoki H, Takada Y, Kondo S, Sawaya R, Aggarwal BB, Kondo Y (2007) Evidence that curcumin suppresses the growth of malignant gliomas in vitro and in vivo through induction of autophagy: role of Akt and extracellular signal-regulated kinase signaling pathways. Mol Pharmacol 72:29–39

Bartlett GR (1959) Phosphorus assay in column chromatography. J Biol Chem 234:466–468

Bligh EG, Dyer WJ (1959) A rapid method of total lipid extraction and purification. Can J Biochem Physiol 37:911–917

Botti J, Djavaheri-Mergny M, Pilatte Y, Codogno P (2006) Autophagy signaling and the cogwheels of cancer. Autophagy 2:67–73

Buratta M, Castigli E, Sciaccaluga M, Pellegrino RM, Spinozzi F, Roberti R, Corazzi L (2008) Loss of cardiolipin in palmitate-treated GL15 glioblastoma cells favors cytochrome c release from mitochondria leading to apoptosis. J Neurochem 105:1019–1031

Bustamante E, Morris HP, Pedersen PL (1981) Energy metabolism of tumor cells. Requirement for a form of hexokinase with a propensity for mitochondrial binding. J Biol Chem 256:8699–8704

Cairns RA, Harris IS, Mak TW (2011) Regulation of cancer cell metabolism. Nat Rev Cancer 11:85–95

Castigli E, Arcuri C, Giovagnoli L, Luciani R, Giovagnoli L, Secca T, Gianfranceschi GL, Bocchini V (2000) Interleukin-1β induces apoptosis in GL15 glioblastoma-derived human cell line. Am J Physiol Cell Physiol 279:C2043–C2049

Castigli E, Sciaccaluga M, Schiavoni G, Brozzi F, Fabiani R, Gorello P, Gianfranceschi GL (2006) GL15 and U251 glioblastoma-derived human cell lines are peculiarly susceptible to induction of mitotic death by very low concentrations of okadaic acid. Oncol Rep 15:463–470

Chen Y, McMillan-Ward E, Kong J, Israels SJ, Gibson SB (2007) Mitochondrial electron-transport-chain inhibitors of complexes I and II induce autophagic cell death mediated by reactive oxygen species. J Cell Sci 120:4155–4166

Eom JM, Seo MJ, Baek JY, Chu H, Han SH, Min TS, Cho CS, Yun CH (2010) Alpha-eleostearic acid induces autophagy-dependent cell death through targeting AKT/mTOR and ERK1/2 signal together with the generation of reactive oxygen species. Biochem Biophys Res Commun 391:903–908

Girardi JP, Pereira L, Bakovic M (2011) De novo synthesis of phospholipids is coupled with autophagosome formation. Medical Hypotheses 77:1083–1087

Hailey DW, Kim PK, Satpute-Krishnan P, Rambold AS, Mitra K, Sougrat R, Lippincott-Schwartz J (2010) Mitochondria supply membranes for autophagosome biogenesis during starvation. Cell 141:656–667

Jelluma N, Yang X, Stokoe D, Evan GI, Dansen TB, Haas-Kogan DA (2006) Glucose withdrawal induces oxidative stress followed by apoptosis in glioblastoma cells but not in normal human astrocytes. Mol Cancer Res 4:319–330

Jiang H, White EJ, Conrad C, Gomez-Manzano C, Fueyo J (2009) Autophagy pathways in glioblastoma. Methos Enzymol 453:273–286

Jiang J, Maeda A, Ji J, Baty CJ, Watkins SC, Greenberger JS, Kagan VE (2011) Are mitochondria reactive oxygen species required for autophagy? Biochem Biophys Res Commun 412:55–60

Joy AM, Beaudry CE, Tran NL, Ponce FA, Holz DR, Demuth T, Berens ME (2003) Migrating glioma cells activate the PI3-K pathway and display decreased susceptibility to apoptosis. J Cell Sci 116:4409–4417

Kim JS, Ahn KJ, Kim JA, Kim HM, Lee JD, Lee JM, Kim SJ, Park JH (2008) Role of reactive oxygen species-mediated mitochondrial dysregulation in 3-bromopyruvate induced cell death in hepatoma cells. J Bioenerg Biomembr 40:607–618

Kirkland RA, Adibhatla RM, Hatcher JF, Franklin JL (2002) Loss of cardiolipin and mitochondria during programmed neuronal death: evidence of a role for lipid peroxidation and autophagy. Neuroscience 115:587–602

Klionsky DJ, Abeliovich H, Agostinis P, Agrawal DK, Aliev G et al (2008) Guidelines for the use and interpretation of assays for monitoring autophagy in higher eukaryotes. Autophagy 4:151–175

Ko YH, Pedersen PL, Geschwind JF (2001) Glucose catabolism in the rabbit VX2 tumor model for liver cancer: characterization and targeting hexokinase. Cancer Lett 173:83–91

Ko YH, Smith BL, Wang Y, Pomper MG, Rini DA, Torbenson MS, Hullihen J, Pedersen PL (2004) Advanced cancers: eradication in all cases using 3-bromopyruvate therapy to deplete ATP. Biochem Biophys Res Commun 324:269–275

Kondo Y, Kanzawa T, Sawaya R, Kondo S (2005) The role of autophagy in cancer development and response to therapy. Nat Rev Cancer 5:726–734

Krakstad C, Chekenya M (2010) Survival signaling and apoptosis resistance in glioblastomas: opportunities for targeted therapeutics. Molecular Cancer 9:135–148

Lefranc F, Kiss R (2006) Autophagy, the Trojan horse to combat glioblastomas. Neurosurg Focus 20:E7

Lefranc F, Facchini V, Kiss R (2007) Proautophagic drugs: a novel means to combat apoptosis-resistant cancers, with a special emphasis on glioblastomas. Oncologist 12:1395–1403

Levine AJ, Puzio-Kuter AM (2010) The control of the metabolic switch in cancers by oncogenes and tumor suppressor genes. Science 330:1340–1344

Lobasso S, Lopalco P, Angelini R, Baronio M, Fanizzi FP, Babudri F, Corcelli A (2010) Lipidomic analysis of porcine olfactory epithelial membranes and cilia. Lipids 45:593–602

Macchioni L, Corazzi T, Davidescu M, Francescangeli E, Roberti R, Corazzi L (2010) Cytochrome c redox state influences the binding and release of cytochrome c in model membranes and in brain mitochondria. Mol Cell Biochem 341:149–157

Macchioni L, Davidescu M, Sciaccaluga M, Marchetti C, Migliorati G, Coaccioli S, Roberti R, Corazzi L, Castigli E (2011a) Mitochondrial dysfunction and effect of antiglycolytic bromopyruvic acid in GL15 glioblastoma cells. J Bioenerg Biomembr 43:507–518

Macchioni L, Davidescu M, Mannucci R, Francescangeli E, Nicoletti I, Roberti R, Corazzi L (2011b) H_2O_2 disposal in cardiolipin-enriched brain mitochondria is due to increased cytochrome c peroxidase activity. Biochim Biophys Acta 1811:203–208

Mathupala SP, Ko YH, Pedersen PL (2006) Hexokinase II: cancer's double-edged sword acting as both facilitator and gatekeeper of malignancy when bound to mitochondria. Oncogene 25:4777–4786

Meloche HP (1967) Bromopyruvate inactivation of 2-keto-3-deoxy-6-phpsphogluconic aldolase. I. Kinetic evidence for active site specificity. Biochemistry 6:2273–2280

Meloche HP, Luczak MA, Wurster JM (1972) The substrate analog, bromopyruvate, as both a substrate and alkylating agent for 2-keto-3-deoxy-6-phpsphogluconic aldolase. Kinetic and stereochemical study. J Biol Chem 247:4186–4191

Pastorino JG, Hoek JB (2008) Regulation of hexokinase binding to VDAC. J Bioenerg Biomembr 40:171–182

Pastorino JG, Hoek JB, Shulga N (2005) Activation of glycogen synthase kinase 3beta disrupts the binding of hexokinase II to mitochondria by phosphorylating voltage-dependent anion channel and potentiates chemotherapy-induced cytoxicity. Cancer Res 65:10545–10554

Pedersen PL (1978) Tumor mitochondria and the bioenergetics of cancer cells. Progr in Exp Tumor Res 22:190–274

Pedersen PL (2007) Warburg, me and hexokinase 2: multiple discoveries of key molecular events underlying one of cancers' most common phenotypes, the "Warburg effect", i.e., elevated glycolysis in the presence of oxygen. J Bioenerg Biomembr 39:211–222

Pedersen PL (2008) Voltage dependent anion channels (VDACs): a brief introduction with a focus on the outer mitochondrial compartment's roles together with hexokinase-2 in the "Warburg effect" in cancer. J Bioenerg Biomembr 40:123–126

Pereira da Silva AP, El-Bacha T, Kyaw N, dos Santos RS, da Silva WS, Almeida FCL, Da Poian AT, Galina A (2009) Inhibition of energy-producing pathways of HepG2 cells by 3-bromopyruvate. Biochem J 417:717–726

Qin J-Z, Xin H, Nickoloff BJ (2010) 3-Bromopyruvate induces necrotic cell death in sensitive melanoma cell lines. Biochem Biophys Res Commun 396:495–500

Sciaccaluga M, Fioretti B, Catacuzzeno L, Pagani F, Bertollini C, Rosito M, Catalano M, D'Alessandro G, Santoro A, Cantore G, Ragozzino D, Castigli E, Franciolini F, Limatola C (2010) CXCL12-induced glioblastoma cell migration requires intermediate conductance Ca^{2+}-activated K^+ channel activity. Am J Physiol Cell Physiol 299:C175–184

Sorice M, Circella A, Cristea IM, Garofalo T, Di Renzo L, Alessandri C, Valesini G, Degli Esposti M (2004) Cardiolipin and its metabolites move from mitochondria to other cellular membranes during death receptor-mediated apoptosis. Cell Death Differ 11:1133–1145

Sun G, Yang K, Zhao Z, Guan S, Han X, Gross RW (2008) Matrix-assisted laser desorption/ionization time-of-flight mass spectrometric analysis of cellular glycerophospholipids enabled by multiplexed solvent dependent analyte-matrix interactions. Anal Chem 80:7576–7585

Vladimirov YA, Proskurnina EV, Izmailov DY, Novikov AA, Brusnichkin AV, Osipov AN, Kagan VE (2006) Cardiolipin activates cytochrome c peroxidase activity since it facilitates H_2O_2 access to heme. Biochem Mosc 71:998–1005

Wang J, Whiteman MW, Lian H, Wang G, Singh A, Huang D, Denmark T (2009) A non-canonical MEK/ERK signaling pathway regulates autophagy via regulating Beclin 1. J Biol Chem 284:21412–21424

Xu R-H, Pelicano H, Zhou Y, Carew JS, Feng L, Bhalla KN, Keating MJ, Huang P (2005) Inhibition of glycolysis in cancer cells: a novel strategy to overcome drug resistance associated with mitochondrial respiratory defect and hypoxia. Cancer Res 65:613–621

Yun J, Rago C, Cheong I, Pagliarini R, Angenendt P, Rajagopalan H, Schmidt K, Willson JK, Markowitz S, Zhou S, Diaz LA Jr, Velculescu VE, Lengauer C, Kinzler KW, Vogelstein B, Papadopoulos N (2009) Glucose deprivation contributes to the development of KRAS pathway mutations in tumor cells. Science 325:1555–1559

Zhang M, Mileykovskaya E, Dowhan W (2002) Gluing the respiratory chain together. Cardiolipin is required for supercomplex formation in the inner mitochondrial membrane. J Biol Chem 277:43553–43556